



Potentially toxic elements and lead isotopic signatures in the 10 μm fraction of urban dust: Environmental risk enhanced by resuspension of contaminated soils

Annapaola Giordano^a, Mery Malandrino^{b,*}, Franco Ajmone Marsan^a, Elio Padoan^a

^a Department of Agricultural, Forest and Food Sciences, University of Turin, Grugliasco, I-10095, Italy

^b Department of Chemistry, University of Turin, Turin, I-10125, Italy

ARTICLE INFO

Keywords:

Potentially toxic element
Urban soil dust
Road dust
Resuspension system
Lead isotopic ratios
Source apportionment

ABSTRACT

In urban environments, soils are a sink of pollutants and might become a source of contamination, as they commonly display potentially toxic elements (PTE) concentrations above the legislative limits. Particularly, the inhalable fraction of soils ($<10 \mu\text{m}$) is enriched in PTE compared to bulk soils (BS). The enrichment makes these particles an environmental hazard because of their susceptibility to resuspension and their potential contribution to road dust (RD) and atmospheric particulate matter (PM₁₀) pollution.

To gain a better insight into urban contamination dynamics we studied the BS, the resuspended $<10 \mu\text{m}$ fraction of BS (Res-BS) and RD (Res-RD) in a European historically industrialized and densely populated city. Compared to BS, the Res-BS and Res-RD showed higher PTE concentrations and a higher variability for most of the elements. Lead was the only PTE showing similar concentrations in all the matrices, suggesting shared sources and redistribution pathways within the city. Chemometric elaborations identified Res-BS as a transition between BS and Res-RD or, rather, a Res-RD precursor. Also, Pb was confirmed to be ubiquitous in all the media.

In all the matrices, Pb isotopic signatures were investigated and compared with PM₁₀ fingerprints from the same city. The anthropogenic isotopic signature in Res-BS and Res-RD was evident, and samples belonging to neighboring sites showed comparable isotopic ratios. The Res-BS appeared as a key driver for Pb distribution within the city both in Res-RD and in PM₁₀. These results demonstrate the intimate interaction between urban environmental compartments (soil, road dust and PM₁₀), and the active contribution of fine soil fractions to anthropogenic pollution, with relevant policy implications in urban areas since soils were found to contribute directly to air pollution.

1. Introduction

Pollution assessment is particularly demanding in urban areas because of the multiplicity of sources, and we could then try to use the sources interconnection to study them. The urban environment is a complex system, where various anthropogenic activities contribute to the dispersion of metal (loid)s into environmental compartments with different responses to contamination. Various sources of point and diffuse pollution coexist, such as traffic exhaust and non-exhaust emissions, residential heating, waste disposal, industrial activities. These sources emit particulates containing potentially toxic elements (PTE), namely Cd, Cr, Cu, Pb, Ni, Zn, V and Sb, which are directly deposited on soil surfaces, roads, and tree leaves through wet and dry atmospheric

deposition (Luo et al., 2019; Shi et al., 2008). The deposition of these PTE-enriched particulates contributes to soil pollution. It has been indicated that soil fine fractions, particularly the particles $<10 \mu\text{m}$ or finer, exhibits higher PTE accumulation than the coarser fractions due to their higher surface area and higher content of reactive clay minerals and organic matter (Ajmone-Marsan et al., 2008; Padoan et al., 2017). More recently, Kelepertzis et al. (2020) reported the appropriateness of using the soil dust to trace the anthropogenic impact in the industrial area of Volos, Greece, and confirmed the sensitivity of soil fine fraction to anthropogenic contamination in industrial and high-density traffic cities.

Soils, however, behave not only as a sink, but also as a source of pollutants under certain conditions, as fine particles have a higher

* Corresponding author.

E-mail address: mery.malandrino@unito.it (M. Malandrino).

<https://doi.org/10.1016/j.envres.2023.117664>

Received 24 August 2023; Received in revised form 26 October 2023; Accepted 12 November 2023

Available online 28 November 2023

0013-9351/© 2023 The Authors. Published by Elsevier Inc. This is an open access article under the CC BY license (<http://creativecommons.org/licenses/by/4.0/>).

resuspension potential compared to the bulk soil (BS). The dust generated from soil resuspension or from the resuspension of dust particles deposited along road edges and park walkways can influence the elemental concentrations in other urban compartments, contributing to the complexity of the contamination conditions, and enhancing human health risks from PTE exposure (Zahran et al., 2013; Padoan and Amato, 2018; Li et al., 2021a). Road dust (RD) is composed, apart from soil dust, by different particles transported and suspended by vehicles or wind, including brake, tire, road wear particles and other particles from various origins (salt, sand, exhaust emissions, secondary compounds, other mineral dust, etc.) (Padoan and Amato, 2018). In the last years, it has been shown that resuspension, redistribution, and transport of PTE-containing particles from soils and RD contribute significantly to urban particulate matter <math><10\ \mu\text{m}</math> (PM_{10}) in all urbanized areas (Padoan and Amato, 2018). For example, in the city of Milan, located in the Po Valley, one of the most contaminated sites in Europe, the so-called *local dust* (sourced from soil and RD), has been calculated to contribute to PM_{10} more than vehicle exhaust (8% of local dust vs 7% of vehicle exhaust) (Amato et al., 2016).

Similarly to soil dust, RD fine particles (i.e., <math><10\ \mu\text{m}</math>) contain PTE concentrations higher than the bulk material in urban areas, as noticed in previous studies (Padoan et al., 2017; Vlasov et al., 2021). Likewise, Khademi et al. (2019) observed that the fraction <math><10\ \mu\text{m}</math> showed the largest accumulation of PTE in RD in both natural and industrial areas in Murcia city, south-eastern Spain. In urban areas, the average concentration of fine particulate matter (PM) is more than twice higher than in rural areas, often exceeding allowable levels with a higher percentage of the population exposed. PM_{10} is classified as a carcinogen to humans by the International Agency for Research on Cancer (IARC) (IARC Scientific Publication No. 161). Particulate pollution has a significant impact on public health and the environment: short-term exposure to particulate air pollution can trigger acute health events, leading to higher rate of emergency department accesses, especially when associated with high air temperatures; long-term exposure increases the risk of cardiovascular and respiratory diseases and reduces life expectancy (Contiero et al., 2019). In 2015, diseases attributable to air pollution caused 18 million deaths worldwide (Roth et al., 2017), with Italy recording 239,514 deaths in the same year (World Health Organization Mortality Database.).

Several studies have been conducted on the PTE accumulation in the fine fraction of sources contributing to PM_{10} in the urban environment. However, most of them consider a single environmental compartment without observing the interdependence among them. In addition, most of the research is limited to the observation of the instantaneous potential emission (Pachon et al., 2021), neglecting the physical process of particle fragmentation and breakdown that occur in urban exposure scenario. Such mechanical processes may cause larger particle size reduction that could further contribute to PM_{10} by affecting the mechanisms of PTE accumulation, transport, and exposure in urban context.

Among PTE, Pb is one of the most widespread in urban settings due to its historical use as gasoline additive (Facchetti, 1989; Wu et al., 2017), and its presence in various industrial emissions. Although no longer used in gasoline, Pb is still considered important in urban areas due to its persistence and neurotoxicity (Becker et al., 2022; Gelly et al., 2019; Morton-Bermea et al., 2011). In the last years the remobilization of this historically deposited Pb has been suggested as an important source of pollution due either to soil resuspension from wind and vehicle movements, or to Pb transport to drainage systems by storm water runoff (Becker et al., 2022; Laidlaw and Filippelli, 2008).

Pb isotope ratios (IRs) remain unchanged throughout physico-chemical and atmospheric processes (Li et al., 2018). Accordingly, in surface soils or RD, Pb signature of anthropogenic and natural sources is preserved in the IRs and could be used as a *fingerprint* to identify and trace Pb pollution sources.

Starting from these considerations, this paper inspects PTE concentrations and Pb isotopic ratio in the bulk soils and in the resuspended

fractions of soils and road dusts with the following aims: i) to clarify the spatial influence of the contamination sources in the urban environment; ii) to evaluate the variability of PTE contents in different urban receptors; iii) to distinguish the natural from anthropogenic origin of Pb and trace its source routes via isotopic ratio study twenty years after the phasing out of leaded gasoline; iv) to investigate the interconnection of urban receptors by focusing on <math><10\ \mu\text{m}</math> resuspended fraction for a better insight of the drivers that contribute to the PTE accumulation and subsequent exposure.

2. Materials and methods

2.1. Study area

Turin is located at the western end of the Po Valley (45°04'24" N; 7°40'32" E), one of the most industrialized areas in Europe. It is a densely populated city with a high volume of vehicular traffic. For more than a century, the economy of Turin province has been strongly linked to industry, particularly to mechanical manufacturing, which has its strong focus on automotive production and all the ancillary industries related to it. The marked presence of the automotive sector has resulted in one of the highest engine rates in Italy, with 664 cars per 1000 inhabitants. In fact, the transport fleet is dominated by cars (44%), using a prevalence of gasoline (48%) and diesel (40%) fuel. Public transport is used for 10% of the urban movements and is characterized by a large and widespread tram network (Berrone et al., 2019). According to Köppen classification, Turin has a warm temperate climate (Cfa); in the last decades, the rainy days are decreasing, consequently increasing the maximum length of dry periods (Arpa Piemonte, 2016). The average annual temperature is about 10 °C, with an average temperature anomaly of about +1.3 °C compared with 1971–2000 data. The Po Valley is characterized by a morphological conformation negatively influencing the pollutants dispersion, worsening its air quality (Padoan et al., 2016). In fact, frequent periods of high pollution occur, during which PM_{10} concentrations exceed the daily average limit of 50 $\mu\text{g}/\text{m}^3$ set by the Directive 2008/50/EC (Implementation of the Directive 2008/50/EC of the European Parliament and of the Council of 21 May 2008 on ambient air quality and cleaner air for Europe, adopted in Italy 2010, 2008). On average, in last years, the daily average has exceeded 100 days per year, against a limit of 35 times per year.

2.2. Sampling and resuspension

The sampling sites were chosen to encompass the variability of the pollution sources in an urban context. BS and RD samples were collected in areas with different traffic densities and in parks within the urban and suburban area of Torino (Fig. 1) as in Padoan et al. (2017). Previous studies (Biasioli et al., 2006; Li et al., 2021b) have shown that these locations are the most representative of soil pollution in Turin for both traffic areas and parks, for their long exposure to airborne diffuse contamination. In addition, two roadside soils sampled (samples ID: 15; 16) in the early 2000s were selected from a previous work (Biasioli et al., 2006) with the aim to observe the isotopic signature of gasoline in soils samples before the leaded gasoline phasing out. These are referred to as *historical samples*.

BS and RD were sampled in the same area when possible, following the methodology described in Padoan et al. (2017). In total, 20 soil sites and 17 road dust sites were selected for this work.

To examine steady-state conditions of deposition, sampling was done after one week without precipitations (Amato et al., 2012). For BS samples, three subsamples were collected at 1 m from each other along the road edge at the same distance from the curb and mixed into a single composite sample. Surface soils (0–5 cm) were considered for the current study because they are more easily resuspended. For RD, three subsamples were collected from sites of 1 m^2 using a polyethylene brush, carefully avoiding re-suspension. For sites belonging to the traffic

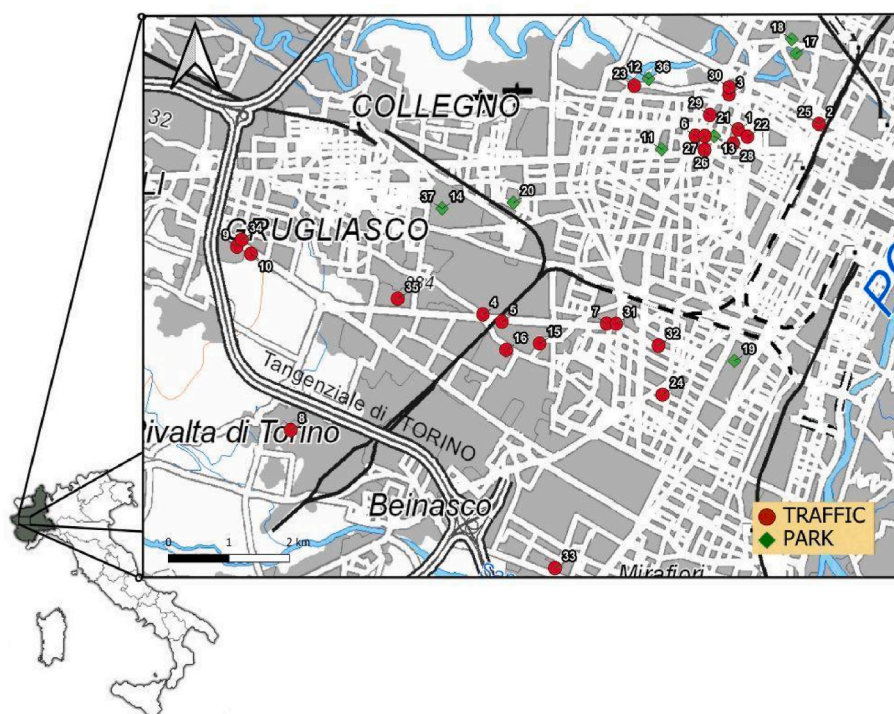


Fig. 1. Map of the sampling sites within Turin urban area, Italy. Traffic sites are represented by red circles, parks by green rhombuses. The numbers represent the samples ID referred to in the text and reported in [Table S1](#).

category, RD samples were sampled at the center of the rightmost active lane. For those in parks at the center of the paved way. All samples were dried at room temperature and sieved to 2 mm.

The fraction <10 of all samples was separated using the equipment illustrated in [Fig. 2](#). The samples analyzed were: 20 bulk soils (BS), 20 samples obtained by resuspension of BS (Res-BS), and 17 samples obtained by resuspension of RD (Res-RD). In the Supplementary Material ([Table S1](#)) the sample list is reported, with coordinates, categorization, and relevant traffic flow.

Starting from the small rotating drum in [Padoan et al. \(2021\)](#), we built a closed metal-free setup to directly sample the PM₁₀ fraction produced by resuspension of the sample without dimensional pretreatment. The experiment was conducted using 15 g of dry BS or RD placed in the rotating drum and revolved at 26 rpm for 1 h. The fall of the sample generates separation of finer particles and additional fine particles are produced from the collision between the particles and the

impact with the chamber wall ([Mendez et al., 2013](#)). Dust particles are transported to the deposition chamber by the vacuum pump located downstream of the system. The deposition chamber allows the deposition of the larger and heavier particles that would damage the PM impactor, avoiding any size pre-treatment. Particles <10 μm are collected on a micro-quartz fiber filter (47 mm, Ahlstrom-Munksjö) using a multistage impactor (MSI, TCR TECORA) according to the ISO 23210-2009 method. Each filter was weighed on an analytical balance (Sartorius CP225D-OCE) before and after the resuspension to calculate the dust load.

2.3. Analytical procedures

BS, Res-BS and Res-RD samples were characterized for pseudo-total elemental concentrations using *aqua regia* extraction and microwave digestion (Milestone Ethos D, ISO 54321:2020). Duplicate extractions

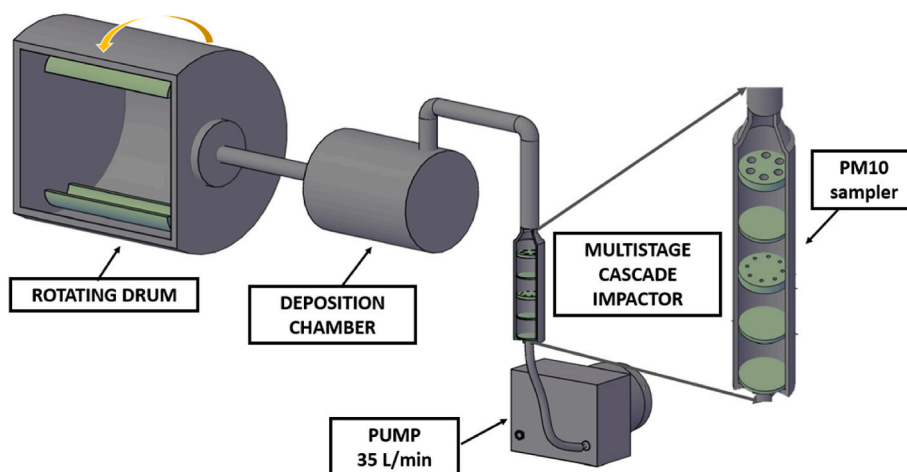


Fig. 2. Scheme of the resuspension system. On the right, an enlargement of multistage cascade impactor to show the PM₁₀ collector.

were performed using 0.2 g of soil sample, ground to 0.15 mm, and 10 mL of *aqua regia*. For the resuspended samples, the entire filter was mineralized. The following heating steps were applied: 10 min ramp until 200 °C, 10 min dwell at 200 °C, and 20 min of ventilation. The resulting solutions were filtered on cellulose filters (Whatman N°41) and diluted to 50 mL with deionized water. Accuracy was verified using a certified reference material for *aqua regia* soluble contents using CRM 141 R certified soil (Community Bureau of Reference, Geel, Belgium); average recovery was 97.9 % (94–103 %). All reagents were of ultrapure or analytical grade. The concentrations of Al, Cd, Cr, Cu, Fe, Ni, Pb, Sb, V and Zn were determined using an Inductively Coupled Plasma Optical Emission Spectroscopy (ICP-OES), Agilent 5800, and an Inductively Coupled Plasma Mass Spectrometer (ICP-MS), Agilent 7500ce.

The Pb relative isotopic composition was determined for the ^{204}Pb , ^{206}Pb , ^{207}Pb , and ^{208}Pb isotopes, using a Sector Field Inductively Coupled Plasma Mass Spectrometer (SF-ICP-MS, Thermo Finnigan Element 2). To obtain a precise and accurate assessment the dependence of analytical precision and accuracy was studied by going to investigate integration window, sapling points per peak and integration times, with the use of face-centered composite experimental design. The SF-ICP-MS obtained operating conditions for Pb isotope analysis are reported in Table S2. More details are given in Ziegler et al. (2021). The determination was performed using the low-resolution mode, using two standard solutions of the certified reference material (CRM) SRM 981 (Common Lead NIST, USA) at concentrations of 2.4 and 24 $\mu\text{g/L}$. The correction for mass bias was performed analyzing the SRM 981 every six samples.

The CRM consists of four isotopes and reflect the Pb natural isotopic abundance: 204 ($1.4255 \pm 0.0012\%$), 206 ($24.1442 \pm 0.0057\%$), 207 ($22.0833 \pm 0.0027\%$), 208 ($52.347 \pm 0.0086\%$). The counts of each isotope were obtained by subtracting the blank signal. On the ^{204}Pb isotope, the interference of ^{204}Hg was subtracted. Considering the natural abundance of the different Hg isotopes, the mathematical correction of the interference of ^{204}Hg was calculated by determining the isotope ^{200}Hg , free from interferences.

2.4. Statistical analyses and data processing

Statistical analyses were conducted using RStudio software (R version 4.0.3) and XLStat 2023. Normality and homoscedasticity of the data were checked using Shapiro-Wilk's and Levene's tests. Non-normal data were log-scaled. One-way ANOVA was used to detect differences in mean values between groups. Tukey-HSD test was applied for *post hoc* pairwise comparisons. Correlation matrices were computed using the non-parametric Spearman method.

To identify the main PTE sources and their contribution to the composition of the different media, principal component analysis (PCA) was applied. Factors were distinguished by the magnitude of factor loadings. Matrices adopted for PCA were scaled and centered before performing the analysis and generating biplots.

Enrichment Factors (EFs) were calculated using the following formula:

$$EF = \left(\frac{C_i/C_r}{C_i/C_r} \right)_{\text{sample}} / \left(\frac{C_i/C_r}{C_i/C_r} \right)_{\text{background}}$$

where $(C_i/C_r)_{\text{sample}}$ and $(C_i/C_r)_{\text{background}}$ are the ratios between the concentration of the *i*-element and the concentration of the reference element in the sample, and in the background soil, or in the Earth's upper crust.

We computed the EFs according to the background values in Turin soils for Cr, Cu, Ni, Pb, Sb, V, and Zn using Fe as reference element because only for these elements regional background levels were available. These values were calculated from the Regional Agency for Environmental Protection according to ISO 19258/2005 norms (ARPA Piemonte, 2015). For Cd, values from the Upper Crust (Wedepohl, 1995)

were used instead.

Iron was used as a reference element because the use of local background concentration might be the best strategy to reduce the distortion induced in EFs calculation from the typical use of average values of rocks or Upper Crust (Bern et al., 2019).

There are no generally accepted grades for the EFs. In this study, we used EFs levels according to Vlasov et al. (2021): <2 depletion to minimal enrichment, 2–5 moderate enrichment; 5–20 significant enrichment and pollution; 20–40 very high enrichment and pollution, and >40 extreme enrichment and pollution.

3. Results and discussion

3.1. PTE distribution in BS, Res-BS, and Res-RD

Descriptive statistics regarding PTE in samples are reported in Table S3 of the Supplementary Material. Data for Al, Cd, Cr, Cu, Fe, Ni, Pb, Sb, V and Zn is reported in Table S4.

In line with the findings of previous studies on Turin soils, high concentrations of all the elements were found through the city area (Ajmone-Marsan et al., 2008; Padoan et al., 2017; Li et al., 2021b). However, no significant differences (at $p = 0.05$) were found in BS samples between park and roadside soils (Fig. 3). Iron and Al are abundant metals found as minerals in the soil; apart from their lithogenic origin, they may also be released into the environment in much lower concentrations by anthropogenic activities. However, given their abundant presence in the soil, both were considered as typical geogenic markers in this study. Traffic soils had averages exceeding the tabulated values for Cr, Ni, Pb and Zn, with some samples also having Sb and Cu concentrations higher than the legislative limits for residential areas. The high concentrations of Cr and Ni could be ascribed to the presence in the soil parent material of ultramafic rocks, such as serpentinitic peridotites and serpentinites, as reported in previous studies in the same area (Biasioli et al., 2006) and in the Regional Environmental Protection Agency study (ARPA Piemonte, 2020) that consistently supported the hypothesis that the high concentrations of these elements were related to the area-specific pedogenesis, lithological composition and prevailing physico-chemical conditions. Vanadium had the lowest variability among studied PTE, while Pb and Sb had the highest. Lead, Sb, Cu, and Zn, in urban areas, have their main sources related to anthropic activities, and it is noticeable that the relative standard deviation (RSD%), was considerably higher in soils located in traffic areas for Pb, Zn, and Sb.

Park soils had, in general, lower PTE concentrations than traffic ones. On average, Ni was the only element slightly exceeding the Italian legislative limit for residential and park sites (D.Lgs. 152/2006), while, looking at the maximum values, Cr and Zn also exceeded the limits in some park samples.

This variability within the city reflects the diverse, intermittent, and long-term effects of human activities on the urban environment, causing highly localized variations in metal concentrations and often preventing the possibility to discriminate soils according to the current land use.

Compared to cities with a similar industrial history, Turin's soils had higher PTE concentrations (Table S5). Notable is the high concentration of Zn and Pb in all the cities, probably because of a convergence of geochemical substrata and pollution sources, as metallurgical industries, and traffic.

Res-BS samples (descriptive statistics reported in Table S3) display two to eight times higher average concentrations and higher variability than BS samples in both parks and traffic areas, suggesting a homogeneity of sources affecting both areas. Antimony and V are the elements showing the highest enrichments in Res-BS. While Sb is emitted mainly from brake and tire wear (Grigoratos and Martini, 2015), V is emitted from metallurgical works, combustion of fuel oil, coal, and diesel vehicles (Zhang et al., 2023) pointing to a diffuse, long-term accumulation of V in the fine fraction of soils. In traffic sites, Cr, Zn and Pb had the

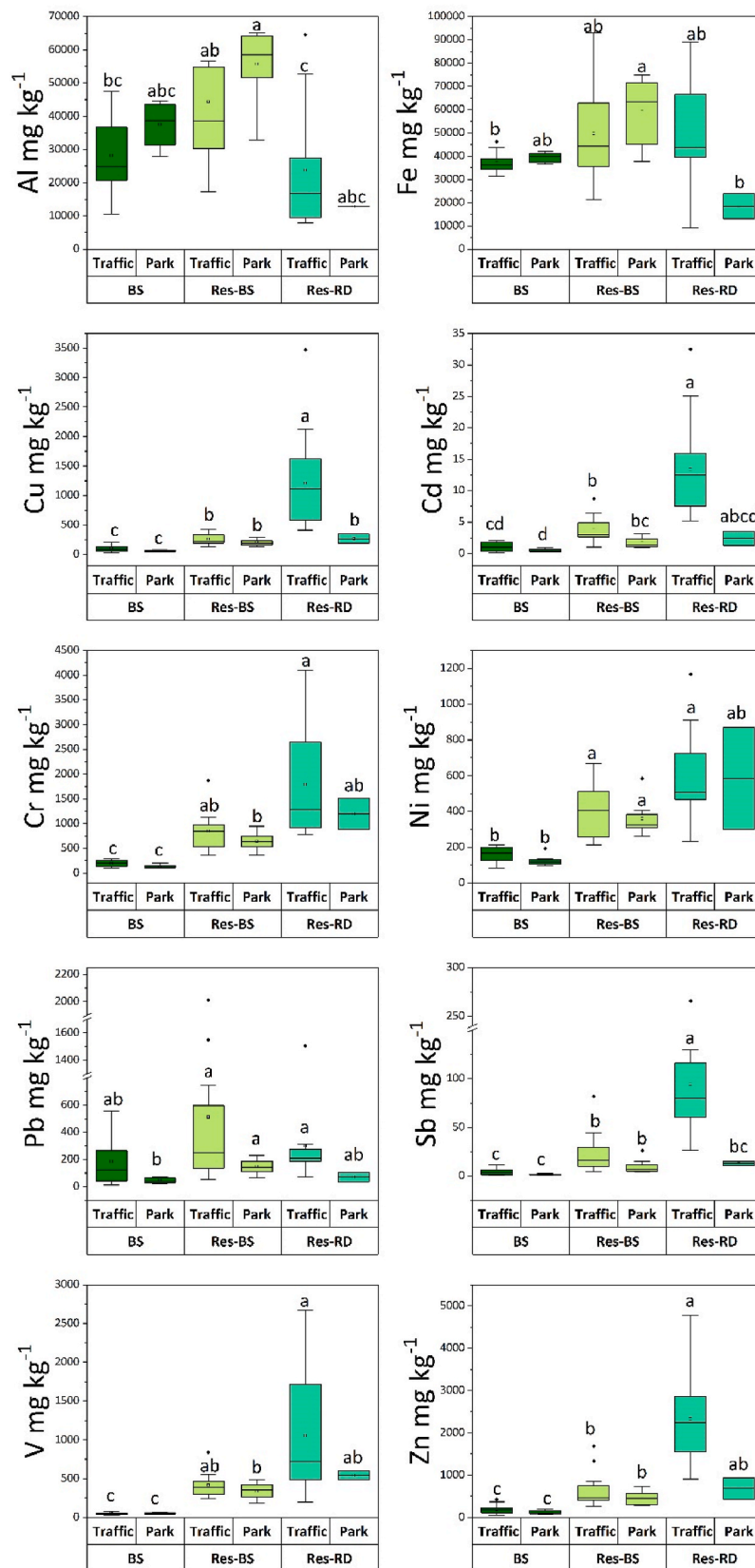


Fig. 3. Elemental concentrations (mg/kg) in the individual matrices (BS, Res-BS and Res-RD) divided by the categories (traffic and park). Superscript letters indicate the statistically significant groups obtained using Tukey-HSD test. The length of the box indicates the interquartile range whereas the horizontal line within each box represents the median. Whiskers indicate minimum and maximum values while outliers are represented as points.

highest concentrations, with Pb having the highest maximum values and RSD% between traffic and park sites, evidencing the long-term influence of Pb diffuse contamination on urban soils twenty years after the phasing out of leaded fuel. Furthermore, all other elements have higher coefficients of variation in traffic than in park sites due to the complexity of the sources at roadside sites. Generally, Res-BS samples displayed lower average concentrations in parks than in traffic sites, with Cr, Zn and Ni showing the highest concentrations, followed by V, Cu and Pb, while Sb had the highest RSD%, evidencing the possible presence of site-specific contaminations.

The various sources present in an urban area contribute to the complexity of the spatial pattern but, in general, Res-BS samples collected in sites with the most trafficked roadways were more contaminated.

Average results for the Res-RD samples are reported in Table S3, while the complete dataset is reported in Table S4. In traffic sites, Res-RD average concentrations of Cd, Cu, Pb, Sb and Zn were high, in line with previous works (Padoan et al., 2017) and with literature studies, if we consider only city centers and industrial areas (Khodadadi et al., 2022; Vlasov et al., 2021). Ni was the only element having similar average concentrations in park and traffic sites, while all other PTE exhibited lower values in parks than in traffic sites. This behavior could

be due to the presence of different prevalent sources in the two land uses (e.g., soil in RD from parks and wear in RD from traffic sites).

Res-RD samples have, generally, higher concentrations and variability than other matrices (as visible in Fig. 3), especially compared to BS, and particularly high concentrations were observed for Cd, Cu, Sb and Zn. The large variability of Res-RD is due to its buildup, as it generates from different materials: soil coming from ridges or roadsides, exhaust emissions, wear of vehicular mechanical parts, asphalt, nearby industrial emissions (Padoan and Amato, 2018). All these sources contribute differently in the different sites, increasing the elemental variability.

Less marked differences between Res-RD and Res-BS were observed for Ni, while for Pb no significant difference was observed in the concentrations of the examined matrices, suggesting shared sources (leaded gasoline and industry) and processes, leading to a similar Pb distribution in urban areas, although with some divergences.

3.2. Enrichment factors

The Enrichment factors (EF) calculated for all samples against local background values are depicted in Fig. 4 as boxplots for each category. In Table S6 all data is reported.

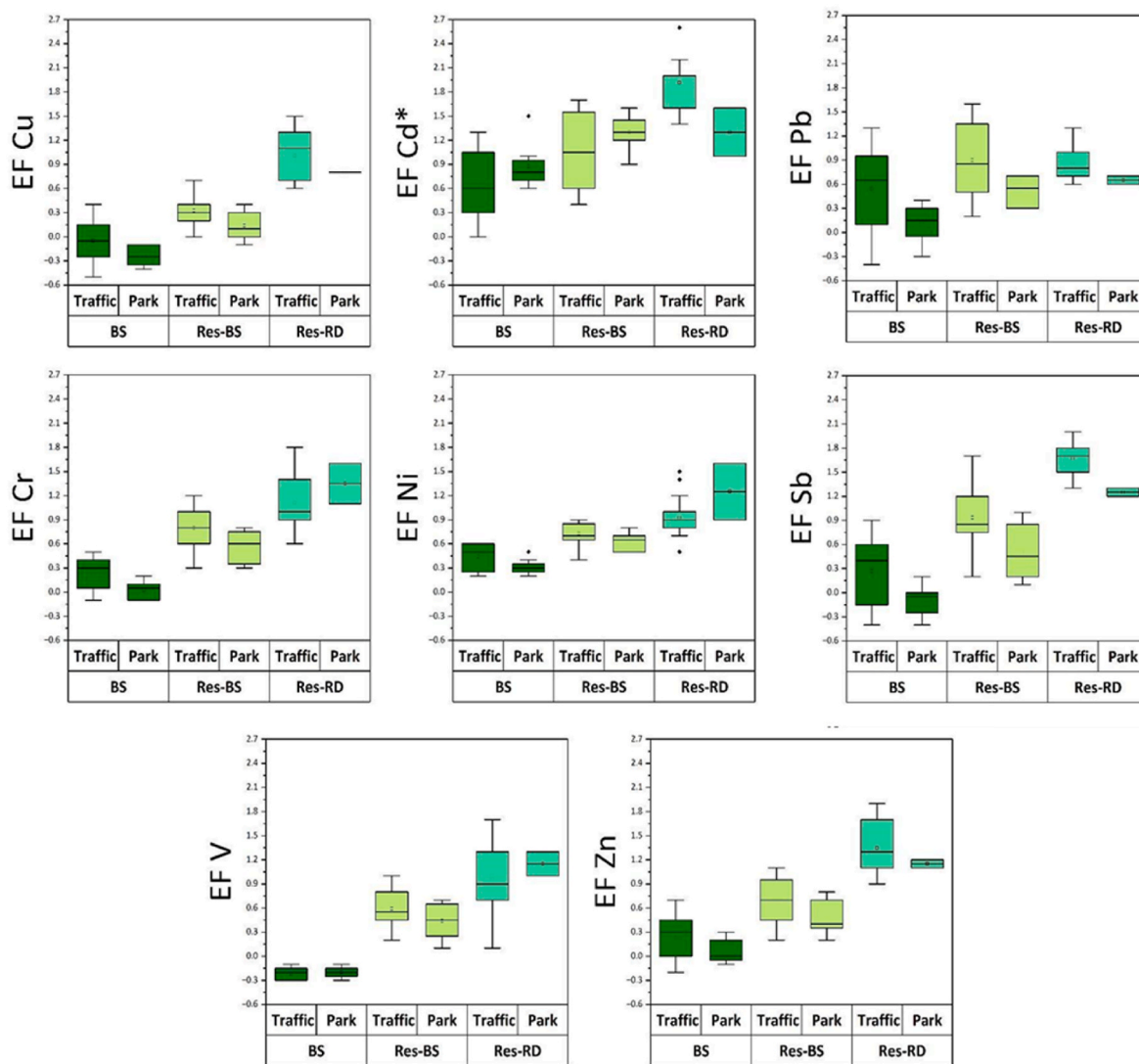


Fig. 4. Enrichment factors calculated for BS, Res-BS, and Res-RD against local background values represented on a logarithmic scale; Fe was used as a reference element. The length of the box indicates the interquartile range whereas the horizontal line within each box represents the median. Whiskers indicate minimum and maximum values, while outliers are represented as points. *Enrichment factors calculated in relation to upper crust values from Wedepohl (1995).

In BS samples, most of the elements displayed a minimal or moderate enrichment. No marked differences are evident comparing EF in park and traffic sites, with Cd having, on average, the highest values. A higher average EF value and variability was observed for Pb and Sb in traffic soils than in parks. The highest EF value was observed for Pb at the sites with highest traffic flow, in large avenues, namely at sites BS4, BS6, and BS10 (EF = 14, 7 and 20 respectively). For the same sites, except for BS4, high EF values were also present for Sb (EF > 8).

Despite their concentrations, the low EF values calculated for Cr and Ni are justified considering their partial lithogenic origin in Turin soils, as previously discussed.

Results for the Res-BS samples are also shown in Fig. 4. Generally, EF values for parks were lower than those for traffic sites, although the complexity of the spatial pattern of sources in urban areas partially overwhelms this simple partition.

In soils located in traffic areas, all elements except Cu exhibited a significant enrichment, especially Cd, Pb and Sb. Significant enrichments of Cr and V were found in four avenues (sites Res-BS1, Res-BS2, Res-BS6 and Res-BS7). The same sites also had extreme and significant enrichments of Sb (EFs = 45, 14, 26, and 7, respectively), likely emitted in road environment during the brake pad wear process (Grigoratos and Martini, 2015). This increase in trafficked sites is related to traffic congestion or tram and bus stops, where vehicles break down more frequently, and it also reflects the vehicles flow intensity (Chang et al., 2021). Accordingly, EF decreased in sites with low vehicular traffic, reaching the lowest values in parks, where EF were always under 5, also observable in Figs. S1(a–e), where the spatial distributions of the EF are shown in relation to traffic flows. Traffic data were obtained from the Piedmont regional geoportal (TGM, 2018).

Local anomalies of Pb and Zn, and significant enrichment of Sb were observed also near industrial zones in sites Res-BS10 (Pb EF = 41; Zn EF = 11; Sb EF = 26) and Res-BS4 (Pb EF = 30; Zn EF = 11; Sb EF = 12). Zinc is emitted during the galvanization process in steel and iron industries to protect iron from rusting (Verma et al., 2020). High Pb values were probably due to the long-term influence of past use of Pb fuels, while Sb originated from vehicle component wear, due to the use of it in brake pads formulation (Grigoratos and Martini, 2015; Pant and Harrison, 2013; Zhu et al., 2020). The presence of anomalies once again confirms the high variability of the distribution of PTE in urban soils.

The high enrichment factors observed in Res-BS may be attributed to its chemico-physical characteristics. Fine particles typically exhibit higher concentrations of metals than coarser ones due to a higher surface area, content of clay minerals and organic matter, and to the presence of Fe–Mn oxide phases acting as PTE sorbents (Ajmone-Marsan et al., 2008). These factors promote the accumulation of metals by co-precipitation, occlusion, adsorption, and complexation.

Among the studied matrices, Res-RD samples were the most enriched in all the selected elements (Fig. 4). Contrarily to Res-BS, for Res-RD land use was a driver. EFs in parks for Cd, Cu, Sb and Zn were markedly lower than in traffic sites, whereas Cr, Ni and V were higher. In traffic sites Cu, Sb and Zn were the most enriched elements, with roadside values nearly twice as high as in parks. Analogously to Res-BS, the high accumulation of Sb and Zn was found in sites with high vehicles flow and frequent stop-start maneuvers and trajectory changes, were intensified tire and brake wear is expected (Alves et al., 2020; Ferreira et al., 2016; Nazzari et al., 2013; Pant and Harrison, 2013). Likewise, Cu is a typical tracer of brake wear emissions, but it also may be emitted by metallurgical plants and machinery companies and can be deposited on the ground from other sources than non-exhaust traffic emissions. In Res-RD samples, the non-exhaust emission is supported from Cu/Sb ratio, averaging 14 in traffic sites, while increasing to 23 in parks. Typical ratios found in Res-RD traffic samples from different cities ranged from 5 to 18 (Alves et al., 2015, 2020; Ramirez et al., 2019). These studies reported that a higher ratio was related to the decrease in Sb concentrations due to the lesser influence of brake wear, suggesting a greater importance of geogenic sources for Cu in parks.

Such high enrichments make particles <10 µm an environmental hazard to citizens due to their susceptibility to resuspension, and their potential to be transported over considerable distances, contributing to urban dust and, atmospheric particulate matter. The Po Valley, of which Piedmont is part, is one of the most polluted areas in Europe, with an estimated 2500 deaths per year in the Piedmont region due to air pollution (VIAS Project). Being surrounded by mountains to the north, west and south, air circulation is limited, causing long periods of stagnant air and, consequently, some of the highest levels of air pollution in Europe (Raaschou-Nielsen et al., 2013; Van Donkelaar et al., 2015). Moreover, the deleterious impact of air pollution also affects animal and plant health, and ecological systems at large (with further consequential impacts on the productivity of agricultural and forestry resources). (World Health Organization. Regional Office for Europe, 2015) Although Europe has made progress in regulating air quality air pollution remains a persistent problem.

3.3. Multivariate analysis

To characterize the underlying contamination sources, we calculated the Spearman's correlation for BS samples (Table S7). A considerable high correlation is appreciable for Cd, Cu, Pb, Zn and Sb, typical urban contaminants in soils. These elements, indeed, relate to traffic (e.g., Cu, Zn and Sb are currently emitted, in urban areas, mostly from brake and tire wear), and to industrial emissions. Activities such as smelting, coal combustion, and construction have been regarded as the major sources of these elements in the environment (Yadav et al., 2019). Moreover, the high correlation between Zn and Cd ($r_{Zn-Cd} = 0.82$; $p < 0.05$) may be an indication of contamination in roadside soils by tire wear. Zinc can be traced, in part, to ZnO used during tire vulcanization process. Cadmium has been associated with impurities in vulcanized tires, as Cd is closely associated with zinc in its natural state (Alves et al., 2020; Pant and Harrison, 2013).

Vanadium shows no correlation with the other elements of interest, indicating a prevalent natural origin. Lastly, the high correlation between Cr and Ni confirms their common origin from the soil geological substrate. However, a contribution from metallurgical activities in Turin cannot be ruled out.

Spearman's correlations were also calculated on Res-BS and Res-RD samples, together with principal component analysis (PCA).

For Res-BS samples, results of the correlations and loadings of the first four components, accounting for the 91% of total variance, are reported in Table 1a and Table S7, respectively. Scores and loadings on the first two PCs are displayed via biplot in Fig. S2. The first component (PC1) is strongly influenced by Cd, Cu, Pb and Zn, elements also showing a high intercorrelation between them, especially in the industrial area and in sites along heavily congested roads. The highly correlated elements Cr and V, conversely, contribute negatively to the second principal component (PC2), suggesting similar sources in the fine fraction, as an anthropic contribution from diffuse sources, i.e., deposition of particulate matter coming from fossil fuel burning or manufacturing activities due to their use in metal alloys that make up engine components (Long et al., 2021). This anthropic addition was presumably hindered in the BS samples from the high natural background. The elements of most likely geogenic origin, Fe and Al, contribute positively to PC2. Park sites are most influenced by the natural component. In fact, these are placed at diffuse values along PC2 and additionally are negatively influenced by the component expressing anthropic elements, confirming for park sites greater influence by elements of natural origin.

Spearman's correlation and PCA analysis were performed also on Res-RD. Correlation results are reported in Table 1(b) while PCA loadings for the first four components, accounting for the 94% of total variance, are reported in Table S9. Scores and loadings on the first and second principal components are displayed via biplot in Fig. S3.

In Res-RD samples, elements of likely anthropogenic origin appear distributed over different components. This behavior is due to the

Table 1

Spearman’s correlation for (a) Res-BS (n = 20) and (b) Res-RD (n = 17) samples. Coefficients are on the upper diagonal; p-value (<0.05) on the lower diagonal. Coefficients higher than 0.6 are in bold.

| (a) | Fe | Al | Cd | Cr | Cu | Pb | Zn | Ni | Sb | V |
|-----|----------|-------------|-------------|-------------|-------------|-------------|-------------|-------------|-------------|-------------|
| Fe | 1 | 0.91 | -0.07 | -0.11 | 0.06 | 0.17 | 0.03 | 0.42 | -0.17 | -0.22 |
| Al | 0.00 | 1 | -0.10 | -0.14 | 0.10 | 0.14 | 0.04 | 0.29 | -0.15 | -0.18 |
| Cd | 0.79 | 0.69 | 1 | 0.70 | 0.87 | 0.54 | 0.59 | 0.33 | 0.49 | 0.59 |
| Cr | 0.63 | 0.55 | 0.00 | 1 | 0.55 | 0.07 | 0.19 | 0.08 | 0.17 | 0.81 |
| Cu | 0.81 | 0.68 | 0.00 | 0.01 | 1 | 0.79 | 0.84 | 0.43 | 0.39 | 0.36 |
| Pb | 0.48 | 0.56 | 0.02 | 0.78 | 0.00 | 1 | 0.94 | 0.56 | 0.21 | -0.20 |
| Zn | 0.91 | 0.88 | 0.01 | 0.44 | 0.00 | 0.00 | 1 | 0.52 | 0.21 | -0.10 |
| Ni | 0.06 | 0.22 | 0.17 | 0.75 | 0.07 | 0.01 | 0.02 | 1 | 0.37 | -0.02 |
| Sb | 0.46 | 0.54 | 0.03 | 0.48 | 0.10 | 0.40 | 0.39 | 0.12 | 1 | 0.52 |
| V | 0.35 | 0.45 | 0.01 | 0.00 | 0.13 | 0.41 | 0.67 | 0.92 | 0.02 | 1 |
| (b) | Fe | Al | Cd | Cr | Cu | Pb | Zn | Ni | Sb | V |
| Fe | 1 | 0.69 | 0.63 | -0.06 | 0.49 | 0.64 | 0.29 | 0.29 | 0.59 | -0.10 |
| Al | 0.02 | 1 | -0.15 | -0.03 | -0.23 | 0.55 | -0.31 | 0.65 | -0.27 | -0.29 |
| Cd | 0.01 | 0.67 | 1 | 0.44 | 0.94 | 0.14 | 0.63 | 0.44 | 0.87 | 0.43 |
| Cr | 0.83 | 0.95 | 0.08 | 1 | 0.53 | 0.15 | 0.53 | 0.61 | 0.40 | 0.99 |
| Cu | 0.05 | 0.49 | 0.00 | 0.03 | 1 | 0.06 | 0.64 | 0.55 | 0.91 | 0.53 |
| Pb | 0.01 | 0.08 | 0.58 | 0.57 | 0.82 | 1 | 0.15 | 0.37 | 0.13 | 0.09 |
| Zn | 0.27 | 0.36 | 0.01 | 0.03 | 0.01 | 0.56 | 1 | 0.19 | 0.61 | 0.56 |
| Ni | 0.28 | 0.03 | 0.08 | 0.01 | 0.02 | 0.15 | 0.46 | 1 | 0.48 | 0.51 |
| Sb | 0.02 | 0.41 | 0.00 | 0.11 | 0.00 | 0.63 | 0.01 | 0.05 | 1 | 0.40 |
| V | 0.71 | 0.39 | 0.08 | 0.00 | 0.03 | 0.75 | 0.02 | 0.04 | 0.11 | 1 |

multiple anthropogenic activities influencing Res-RD production, reflecting the higher variability of Res-RD compared to Res-BS.

Along the first calculated PC, anthropic-derived elements, such as Sb, Cu, Cd, Cr, V and Zn, influenced traffic samples (e.g., Res-RD21, Res-RD22, and Res-RD26) while samples from city parks resulted as not affected. In particular, the Zn and Cu positive correlation was previously found in tramway emissions and railway transport (Vlasov et al., 2021). The emission of all these elements due to vehicle wear is also suggested from the high correlation between Cu, Cd, and Sb ($r_{Cu-Cd} = 0.94$; $r_{Cu-Sb} = 0.91$; $r_{Cd-Sb} = 0.87$). Vanadium and Cr are characterized by positive loadings on PC3, exhibiting a strong correlation between them ($r_{V-Cr} = 0.99$), higher than in Res-BS, probably because of their common sources in soils, in the traffic-derived wear of metallic parts and asphalts, and in the manufacturing activities of metal products.

Aluminum, Fe, Ni and Pb contributed positively to the PC2. The

presence of Pb together with crustal elements suggests also for Pb a soil-derived origin in Res-RD, pointing to contaminated soil dust resuspension as a major origin for Pb in road dust also in Turin, as suggested in previous studies outside Europe (Laidlaw and Filippelli, 2008) but never suggested in Italian sites, to our best knowledge.

Multivariate PCA was performed considering the three matrices grouped (Fig. 5 and Table S10), to observe the distribution of the different matrices in relation to the considered elements. The total cumulative variance of the first two components is 80%. Examining the biplot graph obtained from the multivariate analysis, the characteristic variability of the different matrices is confirmed, as soil have the lowest variance while Res-RD the highest.

The inter-variability between matrices is mainly related to PC2 (related mainly to Fe and Al), with BS samples grouped, indicating common elemental sources. Instead, BS and Res-RD samples are

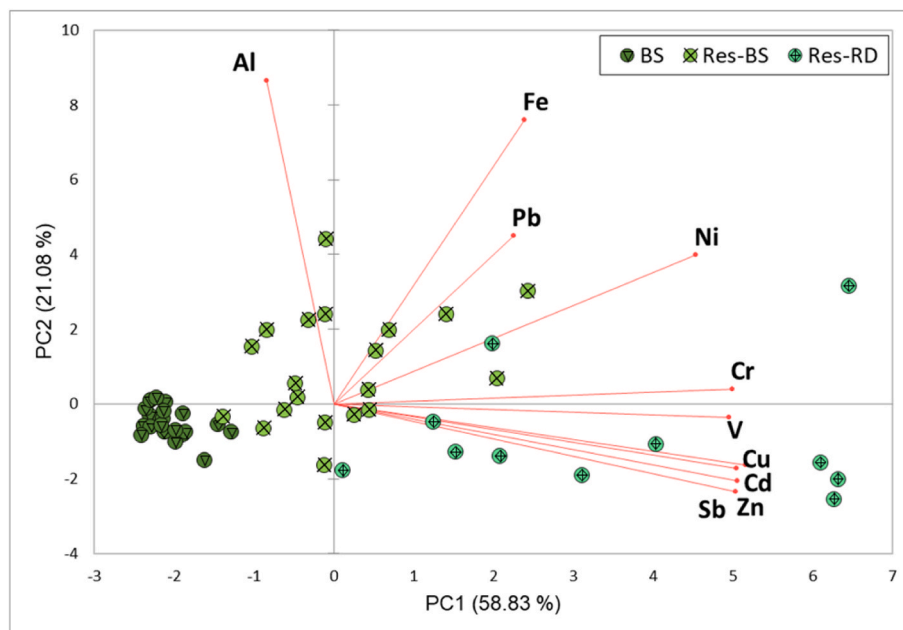


Fig. 5. Biplot graph representing both loadings and scores for PCA obtained considering all the matrices. Data were scaled and centered prior to performing the analysis and generating biplots.

discriminated from PC1 (related to Cd, Cr, Cu, Sb, Zn, V and, to a lower extent, Ni), arising from anthropogenic activities. It is noteworthy to observe that the Res-BS samples appear as a transition between the BS and the Res-RD samples as if to indicate the Res-BS matrix as a precursor in the formation of the fine fraction of RD. This suggests a priority relevance of the composition of Res-BS for proper assessment of citizen health risks. Lead, instead, has the highest loading on PC3. Using PC3, the different matrices were not distinguished, confirming the ubiquity of this element in urban settings and, probably, a common origin in contaminated soils, widespread in historically industrialized towns as Turin.

3.5. Lead isotopic composition

In an attempt to better identify pollution sources, Pb isotope ratios (IRs) were used. Lead has four stable isotopes: 208, 207, 206, and 204; the first three deriving from Th and U radioactive decay, while ^{204}Pb being the only stable isotope with a constant abundance on Earth. Natural materials have, thus, characteristic IRs because of the geological evolution of the area (Doe, 1970). This technique has been used in environmental studies to identify Pb sources in soils, sediments and particulate matter, helping to distinguish the contribution from geological and anthropogenic sources (Gioia et al., 2017; Hansson et al., 2019; Kelepertzis et al., 2020). It can be expressed using different ratios, with the $^{206}\text{Pb}/^{207}\text{Pb}$ ratio being the most preferred because of the relative high abundances of these isotopes.

The idea of historically contaminated soils as main source of Pb in urban settings appeared after the phasing out of leaded gasoline (Laidlaw and Filippelli, 2008) because, in many urban areas, Pb levels in heavily contaminated areas affected blood Pb levels and human health. Twenty years after this event, Pb is still present in soils and RD and, although atmospheric Pb has decreased substantially in European countries, it still has some industrial sources.

In our sites, Pb had strikingly similar concentrations in the different media with no significant difference between BS, Res-BS and Res-RD (Fig. 3). This result suggests a common source in all media and a redistribution pathway from soil to RD through resuspension of fine fraction.

In this study, the $^{206}\text{Pb}/^{207}\text{Pb}$ ratios ranged from 1.117 to 1.121 for traffic BS, while from 1.143 to 1.178 for park BS; from 1.131 to 1.187 for traffic Res-BS, and from 1.127 to 1.174 for park Res-BS. The $^{206}\text{Pb}/^{207}\text{Pb}$

ratios for Res-RD samples ranged from 1.134 to 1.194 for traffic sites, and from 1.147 to 1.157 for park sites (Table S11).

Although the observed differences in IRs are indicative of different relative contributions of common sources to the Pb content of soils and dusts (Bi et al., 2018; Hu et al., 2014), no significant differences were found in the Pb isotopic composition between BS, Res-BS and Res-RD.

The results on all the samples are plotted using the $^{206}\text{Pb}/^{207}\text{Pb}$ and $^{208}\text{Pb}/^{206}\text{Pb}$ ratios in Fig. 6. Such plot highlights Pb sources (Gonzalez et al., 2016; Khondoker et al., 2018). To this aim, different IRs of possible Pb sources (e.g., vehicle exhaust, gasoline and natural sources) from other studies were compared with our results (Gioia et al., 2010, 2017; Lahd Geagea et al., 2008; Facchetti, 1989). In addition, IRs determined in PM_{10} samples collected in Turin (Ziegler et al., 2021) are also plotted.

The first indication arising from Fig. 6 is the overlapping of the ratios of the different media, giving a hint on the mixing processes involving the urban environments. Most of the samples lie in the typical area of traffic sources, suggesting vehicular traffic, historical or present, as main Pb source in all the media. In the same area of the graph are present also Turin PM_{10} samples, in agreement with signatures found in other cities, suggesting that Pb is well mixed within the urban environment.

In soils, the geogenic contribution is characterized by a lower $^{208}\text{Pb}/^{206}\text{Pb}$ ratio (Morton-Bermea et al., 2011), and the natural end member of parent material shows also higher $^{206}\text{Pb}/^{207}\text{Pb}$ ratios compared with the anthropogenic-related sources, as found in previous studies (Kelepertzis et al., 2016, 2020). Traffic sources are, in soil, mixed to Pb coming from the parent material, and to atmospheric particulate matter deposition from anthropogenic activities. Conversely, in Res-RD Pb should derive only from current sources, thus non-exhaust traffic emissions, resuspension of soil dust, and possibly, industrial Pb emissions.

Accordingly, samples in the lowest part of the plot have a greater natural Pb input. In our case, samples in that area are mostly BS from urban parks, while the respective Res-BS samples are positioned in the upper part of the graph. Only one BS from a traffic site (BS9) lies in this area. At this site, Pb concentration was lower than in neighboring traffic sites, likely because the surface had been renovated only some years before the sampling. However, the corresponding Res-BS sample showed a lead isotopic signature comparable with the sites in the same area confirming that, in case of low anthropic contribution, the enrichment is mainly in the soil fine fractions.

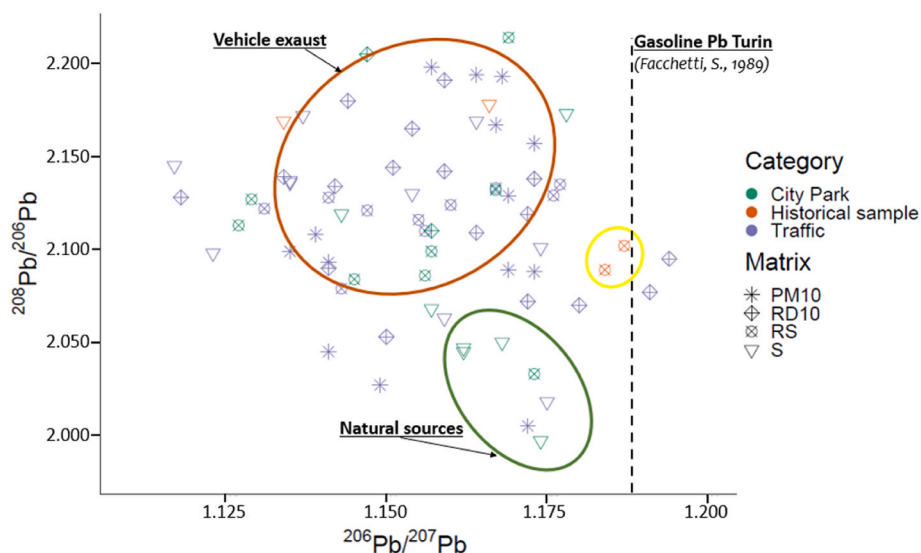


Fig. 6. Isotopic ratios of all the analyzed samples. Circles display ratios of potential anthropogenic sources found in literature: vehicle exhaust (orange circle), gasoline (yellow circle) and natural sources (green circle) (Gioia et al., 2010, 2017; Facchetti, 1989). Ratios of PM_{10} samples collected in Turin are depicted using the asterisk symbol (Ziegler et al., 2021).

In this work, Res-BS and Res-RD sampled in the same area showed comparable Pb isotopic ratios, suggesting that contaminated soil is, indeed, a driving factor of the Pb presence in road dust.

Also, the, PM₁₀ samples of the city of Turin obtained in the work of Ziegler et al. (2021), lie in the range of values found in this work for Res-BS and Res-RD, confirming the interconnection between the different environmental compartments.

As leaded gasoline is thought to be the most important Pb source in urban soils, it is crucial to gather data concerning the origin of gasoline used in studied regions, as Pb isotopic composition was dependent on economic factors, such as the availability and price of Pb ores, and has evolved over time. In the city of Turin, a ten-year study (Facchetti, 1989) was conducted to track Pb used in petrol in the atmosphere by studying Pb isotopic composition. Considering the IR in Turin leaded gasoline ($^{206}\text{Pb}/^{207}\text{Pb} = 1.19$) (Fig. 6), it is evident that all recent samples are far from that level. On the other hand, the isotopic signature of leaded gasoline, can be clearly observed only in the fine fraction of the historical samples, while BS are far from the point.

The fact that only the Res-BS fraction had the characteristic isotopic ratio demonstrates the importance of this fraction for tracing the contribution of lead from anthropogenic activities within the environment.

A second ratio useful for this discrimination is $^{206}\text{Pb}/^{204}\text{Pb}$. Lead of unpolluted soils derives from weathered bedrocks in which the Pb isotopic composition evolved over time reflecting the U/Pb and Th/Pb of the parent material. Lead isotopic signatures of natural soils are thus generally more radiogenic ($^{206}\text{Pb}/^{204}\text{Pb}$: 18.5–19.5) than those of industrial Pb that comes from mining and has a ratio, in Europe, in the range 17.9–18.4 (Doe, 1970).

BS and Res-BS Park samples showed higher $^{206}\text{Pb}/^{204}\text{Pb}$ ratios compared to traffic sites (Table S11), and this trend is confirmed plotting this ratio against the total Pb concentrations (Fig. S4), showing the relation between the highest Pb concentrations and the lowest $^{206}\text{Pb}/^{204}\text{Pb}$ ratios. It is noteworthy that these samples are all Res-BS coming from trafficked areas.

Fig. 7 compares Res-BS and BS averages in park and traffic sites using average normalized element concentrations of Cu, Pb, Zn, Ni and Sb (using Al as normalizing element), and average $^{206}\text{Pb}/^{207}\text{Pb}$ ratios.

As discussed in section 3.1, concentrations of these elements were higher in the Res-BS than in BS, whereas the $^{206}\text{Pb}/^{207}\text{Pb}$ isotopic ratio was lower for Res-BS samples. As evidenced from Fig. 7, sites with a higher anthropogenic Pb input (i.e., traffic sites), had lower $^{206}\text{Pb}/^{207}\text{Pb}$ ratios, while park samples were characterized by higher ratios, attributed to a likely natural origin. Since trace metals tend to accumulate in

fine fractions, the decrease of the ratio indicated the corresponding enrichment of anthropogenic Pb in fine particle fractions of urban soils.

Ultimately, these results highlight the potential risks related to human health via inhalation of Res-BS and Res-RD. Therefore, information on the distribution of PTE in fine fractions should be considered to produce a realistic assessment of the human health risks associated with metals in urban soils.

4. Conclusions

Our research revealed several key findings on pollution dynamics, with a specific focus on the role of fine soil particles contributing to air pollution. The results confirm that PTEs concentrate in fine soil particles and road dust. Although this phenomenon is not new, our research provides additional empirical data, further supporting the idea that fine particles play a central role in an exposure risk scenario. This concentration of PTE has significant implications for the dispersion of pollutants in the environment, particularly in urban areas. Indeed, due to the use of Pb isotopes as effective tracers to identify pollution sources, the clear presence of the anthropogenic isotope signature in the fine fraction below 10 μm (Res-BS and Res-RD) is evident. The overlap of the isotopic ratio in the different environmental media demonstrates the intimate interaction between these environmental compartments and emphasizes the active contribution of fine soil fraction to pollution in urban areas. The complexity of pollution sources in our study area is manifested through a considerable coefficient of variation of isotopic signatures, indicating the impact of both diffuse and point source contamination due to atmospheric deposition of current and past emissions. However, in the resuspended samples, the Pb isotopic signature remains relatively unchanged samples belonging to neighboring sites, while showing the same isotopic signature of leaded gasoline in the historical samples from the early 2000s. These results not only affirm the applicability of Pb isotopes as tracers but underline the complexity of contemporary pollution sources.

These findings have implications for policy makers, as they highlight the significant and underestimated role of soil in the overall contribution to air pollution. Recognizing the importance of soil contamination in the context of air quality management is crucial for designing policies that aim to mitigate air pollution, improve public health, and reduce associated economic and environmental costs. Indeed, air pollution has significant economic and financial implications, impacting not only public health but also productivity and health budgets. Improving air quality can lead to substantial benefits; stricter regulation is therefore necessary.

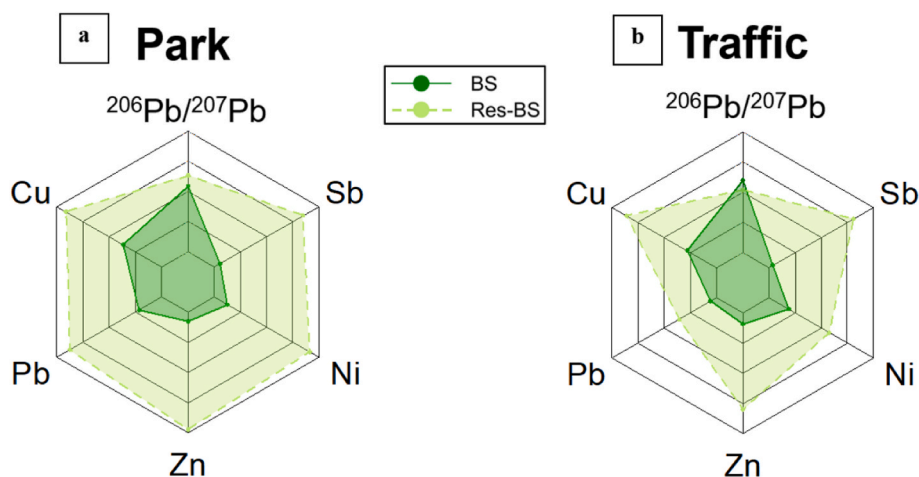


Fig. 7. Comparison between bulk soils (BS) and resuspended fractions $<10\ \mu\text{m}$ (Res-BS) of soils within park (a) and traffic sites (b) using selected variables. In each diagram, average elemental concentrations for each area are normalized using Al to facilitate comparison between BS and Res-BS. The solid line represents average BS data while dashed line average Res-BS data.

Funding information

This work was partly funded by the project “*brAke SyStEmS for future MoBiLiTy improving air quality for Electric and internal combustion engine vehicles*”, ex-Post Project, Compagnia di San Paolo Foundation (Italy), and by MUR ex 60% funds.

CRedit authorship contribution statement

Annapaola Giordano: Conceptualization, Data curation, Formal analysis, Investigation, Writing - original draft, Writing - review & editing. **Mery Malandrino:** Methodology, Formal analysis, Writing - review & editing, Supervision. **Franco Ajmone Marsan:** Conceptualization, Writing - review & editing, Supervision. **Elio Padoan:** Conceptualization, Methodology, Investigation, Writing - review & editing.

Declaration of competing interest

The authors declare that they have no known competing financial interests or personal relationships that could have appeared to influence the work reported in this paper.

Data availability

Data will be made available on request.

Acknowledgements

We wish to thank the three anonymous reviewers who thoroughly revised the manuscript. Following their suggestions, several improvements were included in the present work.

Appendix A. Supplementary data

Supplementary data to this article can be found online at <https://doi.org/10.1016/j.envres.2023.117664>.

References

- Ajmone-Marsan, F., Biasioli, M., Kralj, T., Grčman, H., Davidson, C.M., Hursthouse, A.S., Madrid, L., Rodrigues, S., 2008. Metals in particle-size fractions of the soils of five European cities. *Environ. Pollut.* 152, 73–81. <https://doi.org/10.1016/j.envpol.2007.05.020>.
- Alves, C.A., Gomes, J., Nunes, T., Duarte, M., Calvo, A., Custódio, D., Pio, C., Karanasiou, A., Querol, X., 2015. Size-segregated particulate matter and gaseous emissions from motor vehicles in a road tunnel. *Atmospheric Research* 153, 134–144. <https://doi.org/10.1016/j.atmosres.2014.08.002>.
- Alves, C.A., Vicente, A.M.P., Calvo, A.I., Baumgardner, D., Amato, F., Querol, X., Pio, C., Gustafsson, M., 2020. Physical and chemical properties of non-exhaust particles generated from wear between pavements and tyres. *Atmospheric Environment* 224, 117252. <https://doi.org/10.1016/j.atmosenv.2019.117252>.
- Amato, F., Schaap, M., Denier Van der Gon, H.A.C., Pandolfi, M., Alastuey, A., Keuken, M., Querol, X., 2012. Effect of rain events on the mobility of road dust load in two Dutch and Spanish roads. *Atmos. Environ.* 62, 352e358. <https://doi.org/10.1016/j.atmosenv.2012.08.042>.
- Amato, F., Alastuey, A., Karanasiou, A., Lucarelli, F., Nava, S., Calzolari, G., Severi, M., Becagli, S., Gianelle, V.L., Colombi, C., Alves, C., Custódio, D., Nunes, T., Cerqueira, M., Pio, C., Eleftheriadis, K., Diapouli, E., Reche, C., Minguillón, M.C., Manousakas, M.-I., Maggos, T., Vratolis, S., Harrison, R.M., Querol, X., 2016. AIRUSE-LIFE+: a harmonized PM speciation and source apportionment in five southern European cities. *Atmos. Chem. Phys.* 16, 3289–3309. <https://doi.org/10.5194/acp-16-3289-2016>.
- ARPA Piemonte, 2020. Spazializzazione e valori di fondo naturale delle concentrazioni di Cromo, Nichel e Cobalto nei suoli del comune di Torino e cintura. Deliberazione della Giunta Regionale 2 luglio 2021, n 8–3474.
- Becker, F., Marcantonio, F., Datta, S., Wichterich, C., Cizmas, L., Surber, J., Kennedy, K., Bowles, E., 2022. Tracking the source of contaminant lead in children's blood. *Environ. Res.* 212, 113307. <https://doi.org/10.1016/j.envres.2022.113307>.
- Bern, C.R., Walton-Day, K., Naftz, D.L., 2019. Improved enrichment factor calculations through principal component analysis: examples from soils near breccia pipe uranium mines, Arizona, USA. *Environ. Pollut.* 248, 90–100. <https://doi.org/10.1016/j.envpol.2019.01.122>.
- Berrone, G., Sala, A., Gagliardi, G., Gasparini, C., Tommasi, D., Marinetto, F., 2019. available at: Mobilità Veicolare In Piemonte www.regione.piemonte.it www.5t.torino.it.
- Bi, C., Zhou, Y., Chen, Z., Jia, J., Bao, X., 2018. Heavy metals and lead isotopes in soils, road dust and leafy vegetables and health risks via vegetable consumption in the industrial areas of Shanghai, China. *Sci. Total Environ.* 619, 1349–1357. <https://doi.org/10.1016/j.scitotenv.2017.11.177>.
- Biasioli, M., Barberis, R., Ajmone Marsan, F., 2006. The influence of a large city on some soil properties and metals content. *Sci. Total Environ.* 356, 154–164. <https://doi.org/10.1016/j.scitotenv.2005.04.033>.
- Chang, X., Yu, Y., Li, Y.-X., 2021. Response of antimony distribution in street dust to urban road traffic conditions. *J. Environ. Manag.* 296, 113219. <https://doi.org/10.1016/j.jenvman.2021.113219>.
- Contiero, P., Boffi, R., Tagliabue, G., Scaburri, A., Tittarelli, A., Bertoldi, M., Borgini, A., Favia, I., Ruprecht, A.A., Maiorino, A., Voza, A., Ripoll Pons, M., Cau, A., DeMarco, C., Allegri, F., Tresoldi, C., Ciccarelli, M., 2019. A case-crossover study to investigate the effects of atmospheric particulate matter concentrations, season, and air temperature on accident and emergency presentations for cardiovascular events in northern Italy. *IJERPH* 16, 4627. <https://doi.org/10.3390/ijerph16234627>.
- Doe, B.R., 1970. Lead Isotopes. Springer Berlin Heidelberg, Berlin, Heidelberg. <https://doi.org/10.1007/978-3-642-87280-8>.
- D.Lgs. 152/2006. Gazzetta Ufficiale della Repubblica Italiana, Decreto legislativo 3 aprile 2006, n. 152 Norme in materia ambientale.
- Facchetti, S., 1989. Lead in petrol. The isotopic lead experiment. *Acc. Chem. Res.* 22, 370–374. <https://doi.org/10.1021/ar00166a005>.
- Ferreira, A.J.D., Soares, D., Serrano, L.M.V., Walsh, R.P.D., Dias-Ferreira, C., Ferreira, C.S.S., 2016. Roads as sources of heavy metals in urban areas. The Covões catchment experiment, Coimbra, Portugal. *J Soils Sediments* 16, 2622–2639. <https://doi.org/10.1007/s11368-016-1492-4>.
- Gelly, R., Fekiacova, Z., Guihou, A., Doelsch, E., Deschamps, P., Keller, C., 2019. Lead, zinc, and copper redistributions in soils along a deposition gradient from emissions of a Pb-Ag smelter decommissioned 100 years ago. *Sci. Total Environ.* 665, 502–512. <https://doi.org/10.1016/j.scitotenv.2019.02.092>.
- Gioia, S.M.C.L., Babinski, M., Weiss, D.J., Kerr, A.A.F.S., 2010. Insights into the dynamics and sources of atmospheric lead and particulate matter in São Paulo, Brazil, from high temporal resolution sampling. *Atmos. Res.* 98, 478–485. <https://doi.org/10.1016/j.atmosres.2010.08.016>.
- Gioia, S.M.C.L., Babinski, M., Weiss, D.J., Spiro, B., Kerr, A.A.F.S., Veríssimo, T.G., Ruiz, I., Prates, J.C.M., 2017. An isotopic study of atmospheric lead in a megacity after phasing out of leaded gasoline. *Atmos. Environ.* 149, 70–83. <https://doi.org/10.1016/j.atmosenv.2016.10.049>.
- Gonzalez, R.O., Strelkopytov, S., Amato, F., Querol, X., Reche, C., Weiss, D., 2016. New insights from zinc and copper isotopic compositions into the sources of atmospheric particulate matter from two major European cities. *Environ. Sci. Technol.* 50, 9816–9824. <https://doi.org/10.1021/acs.est.6b00863>.
- Grigoratos, T., Martini, G., 2015. Brake wear particle emissions: a review. *Environ Sci Pollut Res* 22, 2491–2504. <https://doi.org/10.1007/s11356-014-3696-8>.
- Hansson, S.V., Grusson, Y., Chimienti, M., Claustres, A., Jean, S., Le Roux, G., 2019. Legacy Pb pollution in the contemporary environment and its potential bioavailability in three mountain catchments. *Sci. Total Environ.* 671, 1227–1236. <https://doi.org/10.1016/j.scitotenv.2019.03.403>.
- Hu, X., Sun, Y., Ding, Z., Zhang, Y., Wu, J., Lian, H., Wang, T., 2014. Lead contamination and transfer in urban environmental compartments analyzed by lead levels and isotopic compositions. *Environ. Pollut.* 187, 42–48. <https://doi.org/10.1016/j.envpol.2013.12.025>.
- IARC Scientific Publication No. 161: Air Pollution and Cancer [(accessed on 13 September 2019)]; Available online: <http://www.iarc.fr/en/publications/books/sp161/AirPollutionandCancer161.pdf>.
- Implementation of the Directive 2008/50/EC of the European Parliament and of the Council of 21 May 2008 on ambient air quality and cleaner air for Europe, adopted in Italy in 2010, 2008. [https://www.europarl.europa.eu/RegData/etudes/STUD/2016/578986/IPOL_STU\(2016\)578986_EN.pdf](https://www.europarl.europa.eu/RegData/etudes/STUD/2016/578986/IPOL_STU(2016)578986_EN.pdf).
- Keleperizis, E., Komárek, M., Argyraki, A., Šillerová, H., 2016. Metal(loid) distribution and Pb isotopic signatures in the urban environment of Athens, Greece. *Environ. Pollut.* 213, 420–431. <https://doi.org/10.1016/j.envpol.2016.02.049>.
- Keleperizis, E., Argyraki, A., Chrastný, V., Botsou, F., Skordas, K., Komárek, M., Fouskas, A., 2020. Metal(loid) and isotopic tracing of Pb in soils, road and house dusts from the industrial area of Volos (central Greece). *Sci. Total Environ.* 725, 138300. <https://doi.org/10.1016/j.scitotenv.2020.138300>.
- Khademi, H., Gabarrón, M., Abbaspour, A., Martínez-Martínez, S., Faz, A., Acosta, J.A., 2019. Environmental impact assessment of industrial activities on heavy metals distribution in street dust and soil. *Chemosphere* 217, 695–705. <https://doi.org/10.1016/j.chemosphere.2018.11.045>.
- Khodadadi, N., Amini, A., Dehbandi, R., 2022. Contamination, probabilistic health risk assessment and quantitative source apportionment of potentially toxic metals (PTMs) in street dust of a highly developed city in north of Iran. *Environ. Res.* 210, 112962. <https://doi.org/10.1016/j.envres.2022.112962>.
- Khondoker, R., Weiss, D., van de Fliert, T., Rehkämper, M., Kreissig, K., Coles, B.J., Strelkopytov, S., Humphreys-Williams, E., Dong, S., Bory, A., Bout-Roumazeilles, V., Smichowski, P., Cid-Aguero, P., Babinski, M., Losno, R., Monna, F., 2018. New constraints on elemental and Pb and Nd isotope compositions of south American and southern african aerosol sources to the south atlantic ocean. *Geochemistry* 78, 372–384. <https://doi.org/10.1016/j.chemer.2018.05.001>.
- Lahd Geagea, M., Stille, P., Gauthier-Lafaye, F., Millet, M., 2008. Tracing of industrial aerosol sources in an urban environment using Pb, Sr, and Nd isotopes. *Environ. Sci. Technol.* 42, 692–698. <https://doi.org/10.1021/es071704c>.

- Laidlaw, M.A.S., Filippelli, G.M., 2008. Resuspension of urban soils as a persistent source of lead poisoning in children: a review and new directions. *Applied Geochemistry* 23, 2021–2039.
- Li, F., Jinxu, Y., Shao, L., Zhang, G., Wang, J., Jin, Z., 2018. Delineating the origin of Pb and Cd in the urban dust through elemental and stable isotopic ratio: a study from Hangzhou City, China. *Chemosphere* 211, 674–683. <https://doi.org/10.1016/j.chemosphere.2018.07.199>.
- Li, Y., Ajmone-Marsan, F., Padoan, E., 2021a. Health risk assessment via ingestion and inhalation of soil PTE of an urban area. *Chemosphere* 281, 130964. <https://doi.org/10.1016/j.chemosphere.2021.130964>.
- Li, Y., Padoan, E., Ajmone-Marsan, F., 2021b. Soil particle size fraction and potentially toxic elements bioaccessibility: a review. *Ecotoxicology and Environmental Safety* 209, 111806. <https://doi.org/10.1016/j.ecoenv.2020.111806>.
- Long, Z., Zhu, H., Bing, H., Tian, X., Wang, Z., Wang, X., Wu, Y., 2021. Contamination, sources and health risk of heavy metals in soil and dust from different functional areas in an industrial city of Panzhihua City, Southwest China. *J.Hazardous Mater.* 420, 126638 <https://doi.org/10.1016/j.jhazmat.2021.126638>.
- Luo, X., Bing, H., Luo, Z., Wang, Y., Jin, L., 2019. Impacts of atmospheric particulate matter pollution on environmental biogeochemistry of trace metals in soil-plant system: a review. *Environ. Pollut.* 255, 113138 <https://doi.org/10.1016/j.envpol.2019.113138>.
- Mendez, M.J., Panebianco, J.E., Buschiazzi, D.E., 2013. A new dust generator for laboratory dust emission studies. *Aeolian Res.* 8, 59–64. <https://doi.org/10.1016/j.aeolia.2012.10.007>.
- Morton-Bermea, O., Rodríguez-Salazar, M.T., Hernández-Alvarez, E., García-Arreola, M. E., Lozano-Santacruz, R., 2011. Lead isotopes as tracers of anthropogenic pollution in urban topsoils of Mexico City. *Geochemistry* 71, 189–195. <https://doi.org/10.1016/j.chemer.2011.03.003>.
- Nazzari, Y., Rosen, M.A., Al-Rawabdeh, A.M., 2013. Assessment of metal pollution in urban road dusts from selected highways of the Greater Toronto Area in Canada. *Environ Monit Assess* 185, 1847–1858. <https://doi.org/10.1007/s10661-012-2672-3>.
- Pachon, J.E., Vanegas, S., Saavedra, C., Amato, F., Silva, L.F.O., Blanco, K., Chaparro, R., Casas, O.M., 2021. Evaluation of factors influencing road dust loadings in a Latin American urban center. *J. Air & Waste Manag. Assoc.* 71, 268–280. <https://doi.org/10.1080/10962247.2020.1806946>.
- Padoan, E., Amato, F., 2018. Vehicle non-exhaust emissions. In: *Non-Exhaust Emissions*. Elsevier, pp. 21–65. <https://doi.org/10.1016/B978-0-12-811770-5.00002-9>.
- Padoan, E., Malandrino, M., Giacomino, A., Grosa, M.M., Lollobrigida, F., Martini, S., Abollino, O., 2016. Spatial distribution and potential sources of trace elements in PM10 monitored in urban and rural sites of Piedmont Region. *Chemosphere* 145, 495–507. <https://doi.org/10.1016/j.chemosphere.2015.11.094>.
- Padoan, E., Romé, C., Ajmone-Marsan, F., 2017. Bioaccessibility and size distribution of metals in road dust and roadside soils along a peri-urban transect. *Sci. Total Environ.* 602, 89–98. <https://doi.org/10.1016/j.scitotenv.2017.05.180>, 601.
- Padoan, E., Maffia, J., Balsari, P., Ajmone-Marsan, F., Dinuccio, E., 2021. Soil PM10 emission potential under specific mechanical stress and particles characteristics. *Sci. Total Environ.* 779, 146468 <https://doi.org/10.1016/j.scitotenv.2021.146468>.
- Pant, P., Harrison, R.M., 2013. Estimation of the contribution of road traffic emissions to particulate matter concentrations from field measurements: a review. *Atmos. Environ.* 77, 78–97. <https://doi.org/10.1016/j.atmosenv.2013.04.028>.
- Raaschou-Nielsen, O., Andersen, Z.J., Beelen, R., Samoli, E., Stafoggia, M., Weinmayr, G., Hoffmann, B., Fischer, P., Nieuwenhuijsen, M.J., Brunekreef, B., Xun, W.W., Katsouyanni, K., Dimakopoulou, K., Sommar, J., Forsberg, B., Modig, L., Oudin, A., Oftedal, B., Schwarze, P.E., Nafstad, P., De Faire, U., Pedersen, N.L., Ostenson, C.-G., Fratiglioni, L., Penell, J., Korek, M., Pershagen, G., Eriksen, K.T., Sørensen, M., Tjønneland, A., Ellermann, T., Eeftens, P., Peeters, P.H., Meliefste, K., Wang, M., Bueno-de-Mesquita, B., Key, T.J., De Hoogh, K., Concin, H., Nagel, G., Vilier, A., Grióni, S., Krogh, V., Tsai, M.-Y., Ricceri, F., Sacerdote, C., Galassi, C., Migliore, E., Ranzi, A., Cesaroni, G., Badaloni, C., Forastiere, F., Tamayo, I., Amiano, P., Dorronsoro, M., Trichopoulos, A., Bamia, C., Vineis, P., Hoek, G., 2013. Air pollution and lung cancer incidence in 17 European cohorts: prospective analyses from the European Study of Cohorts for Air Pollution Effects (ESCAPE). *The Lancet Oncology* 14, 813–822. [https://doi.org/10.1016/S1470-2045\(13\)70279-1](https://doi.org/10.1016/S1470-2045(13)70279-1).
- Ramírez, O., Sánchez de la Campa, A.M., Amato, F., Moreno, T., Silva, L.F., de la Rosa, J. D., 2019. Physicochemical characterization and sources of the thoracic fraction of road dust in a Latin American megacity. *Sci. Total Environ.* 652, 434–446. <https://doi.org/10.1016/j.scitotenv.2018.10.214>.
- Roth, G.A., Johnson, C., Abajobir, A., Abd-Allah, F., Abera, S.F., Abyu, G., Ahmed, M., Aksut, B., Alam, T., Alam, K., Ailla, F., Alvis-Guzman, N., Amrock, S., Ansari, H., Ärnlöv, J., Asayesh, H., Atey, T.M., Avila-Burgos, L., Awasthi, A., Banerjee, A., Barac, A., Bärnighausen, T., Barregard, L., Bedi, N., Belay Ketema, E., Bennett, D., Berhe, G., Bhutta, Z., Bitew, S., Carapetis, J., Carrero, J.J., Malta, D.C., Castañeda
- Orjuela, C.A., Castillo-Rivas, J., Catalá-López, F., Choi, J.-Y., Christensen, H., Cirillo, M., Cooper, L., Criqui, M., Cundiff, D., Damasceno, A., Dandona, L., Dandona, R., Davletov, K., Dharmaratne, S., Dorairaj, P., Dubey, M., Ehrenkranz, R., El Sayed Zaki, M., Faraon, E.J.A., Esteghamati, A., Farid, T., Farvid, M., Feigin, V., Ding, E.L., Fowkes, G., Gebrehiwot, T., Gillum, R., Gold, A., Gona, P., Gupta, R., Habtewold, T.D., Hafezi-Nejad, N., Hailu, T., Hailu, G.B., Hankey, G., Hassen, H.Y., Abate, K.H., Havmoeller, R., Hay, S.I., Horino, M., Hotez, P.J., Jacobsen, K., James, S., Javanbakht, M., Jeemon, P., John, D., Jonas, J., Kalkonde, Y., Karimkhani, C., Kasaian, A., Khader, Y., Khan, A., Khang, Y.-H., Khra, S., Khoja, A. T., Khubchandani, J., Kim, D., Kolte, D., Kosen, S., Krohn, K.J., Kumar, G.A., Kwan, G.F., Lal, D.K., Larsson, A., Linn, S., Lopez, A., Lotufo, P.A., El Rizek, H.M.A., Malekzadeh, R., Mazidi, M., Meier, T., Meles, K.G., Mensah, G., Meretoja, A., Mezgebe, H., Miller, T., Mirrakhimov, E., Mohammed, S., Moran, A.E., Musa, K.I., Narula, J., Neal, B., Ngallesoni, F., Nguyen, G., Obermeyer, C.M., Owolabi, M., Patton, G., Pedro, J., Qato, D., Qorbani, M., Rahimi, K., Rai, R.K., Rawaf, S., Ribeiro, A., Safiri, S., Salomon, J.A., Santos, I., Santric Milicevic, M., Sartorius, B., Schutte, A., Sepanlou, S., Shaikh, M.A., Shin, M.-J., Shishebor, M., Shore, H., Silva, D.A.S., Sobngwi, E., Stranges, S., Swaminathan, S., Tabarés-Seisdedos, R., Tadele Atmifu, N., Tesfay, F., Thakur, J.S., Thrift, A., Topor-Madry, R., Truelsen, T., Tyrovolas, S., Ukwaja, K.N., Uthman, O., Vasankari, T., Vlassov, V., Vollset, S.E., Wakayo, T., Watkins, D., Weintraub, R., Werdecker, A., Westerman, R., Wiysonge, C. S., Wolfe, C., Workicho, A., Xu, G., Yano, Y., Yip, P., Yonemoto, N., Younis, M., Yu, C., Vos, T., Naghavi, M., Murray, C., 2017. Global, regional, and national burden of cardiovascular diseases for 10 causes, 1990 to 2015. *Journal of the American College of Cardiology* 70, 1–25. <https://doi.org/10.1016/j.jacc.2017.04.052>.
- Shi, G., Chen, Z., Xu, S., Zhang, J., Wang, L., Bi, C., Teng, J., 2008. Potentially toxic metal contamination of urban soils and roadside dust in Shanghai, China. *Environmental Pollution* 156, 251–260. <https://doi.org/10.1016/j.envpol.2008.02.027>.
- TGM, 2018. Average Annual Daily Traffic on Road Element BDTRE. <https://www.regi-one.piemonte.it>.
- Van Donkelaar, A., Martin, R.V., Brauer, M., Boys, B.L., 2015. Use of satellite observations for long-term exposure assessment of global concentrations of fine particulate matter. *Environ Health Perspect* 123, 135–143. <https://doi.org/10.1289/ehp.1408646>.
- Verma, A., Kumar, R., Yadav, S., 2020. Distribution, pollution levels, toxicity, and health risk assessment of metals in surface dust from Bhiwadi industrial area in North India. *Human and Ecological Risk Assessment: An International J.* 26, 2091–2111. <https://doi.org/10.1080/10807039.2019.1650328>.
- VIIAS Project, Metodi per la Valutazione Integrata dell'Impatto Ambientale e Sanitario dell'inquinamento atmosferico <https://www.vvias.it/pagine/impatto-sulla-salute..>
- Vlasov, D., Kosheleva, N., Kasimov, N., 2021. Spatial distribution and sources of potentially toxic elements in road dust and its PM10 fraction of Moscow megacity. *Sci. Total Environ.* 761, 143267 <https://doi.org/10.1016/j.scitotenv.2020.143267>.
- Wedepohl, H.K., 1995. The composition of the continental crust. *Geochimica et Cosmochimica Acta* 59, 1217–1232. [https://doi.org/10.1016/0016-7037\(95\)00038-2](https://doi.org/10.1016/0016-7037(95)00038-2).
- World Health Organization Mortality Database [(accessed on 18 November 2019)]; Available online: <http://apps.who.int/healthinfo/statistics/mortality/whodpms/>.
- World Health Organization. Regional Office for Europe, 2015. Economic Cost of the Health Impact of Air Pollution in Europe: Clean Air, Health and Wealth. World Health Organization. Regional Office for Europe. <https://iris.who.int/handle/10665/350716>.
- Wu, L., Taylor, M.P., Handley, H.K., 2017. Remobilisation of industrial lead depositions in ash during Australian wildfires. *Science of The Total Environment* 599, 1233–1240. <https://doi.org/10.1016/j.scitotenv.2017.05.044>, 600.
- Yadav, I.C., Devi, N.L., Singh, V.K., Li, J., Zhang, G., 2019. Spatial distribution, source analysis, and health risk assessment of heavy metals contamination in house dust and surface soil from four major cities of Nepal. *Chemosphere* 218, 1100–1113. <https://doi.org/10.1016/j.chemosphere.2018.11.202>.
- Zahrán, S., Mielke, H.W., McElmurry, S.P., Filippelli, G.M., Laidlaw, M.A.S., Taylor, M.P., 2013. Determining the relative importance of soil sample locations to predict risk of child lead exposure. *Environ. Intern.* 60, 7–14. <https://doi.org/10.1016/j.envint.2013.07.004>.
- Zhang, B., Zhang, H., He, J., Zhou, S., Dong, H., Rinklebe, J., Ok, Y.S., 2023. Vanadium in the environment: biogeochemistry and bioremediation. *Environ. Sci. Technol.* 57, 14770–14786. <https://doi.org/10.1021/acs.est.3c04508>.
- Zhu, C., Tian, H., Hao, J., 2020. Global anthropogenic atmospheric emission inventory of twelve typical hazardous trace elements, 1995–2012. *Atmospheric Environ.* 220, 117061.
- Ziegler, D., Malandrino, M., Barolo, C., Adami, G., Sacco, M., Pitasi, F., Abollino, O., Giacomino, A., 2021. Influence of start-up phase of an incinerator on inorganic composition and lead isotope ratios of the atmospheric PM10. *Chemosphere* 266, 129091. <https://doi.org/10.1016/j.chemosphere.2020.129091>.